



# Numerical study of TRIP transformation in 35NCD16 steel-effects of plate orientation and some criteria

Mounir Gaci

Laboratory of Mechanics, University Frères Mentouri Constantine 1, Constantine, Algeria  
mounir.gaci@umc.edu.dz

Kamel Fedaoui, Lazhar Baroura

University Frères Mentouri Constantine 1, Constantine, Algeria  
Kamel.fedaoui@umc.edu.dz, <https://orcid.org/0000-0003-0885-6914>  
barouralaz@ yahoo.fr, <https://orcid.org/0000-0002-6747-5049>

Amar Talhi

Metallurgy and Materials Engineering, Foundry laboratory,  
Badji Mokhtar University - Annaba, Algeria  
talhiamaryacine@gmail.com

**ABSTRACT.** This study aims to analyze the effect of thermo mechanical coupling damage in the presence of a phase change (austenite/martensite) in 35NCD16 steel. The impact of increasing mechanical traction load, accompanied by a martensitic transformation on the scale of a single grain with boundary has been studied. The prediction transformation of induced plasticity (TRIP) was evaluated by taking into account the following parameters: twenty shear directions of the martensitic plates, two values of the shear deformation of the martensitic plates, energetic and thermodynamics criteria for getting in order the transformation of the martensitic plates, elastoplastic behavior of the two areas in the first case (martensitic plate and grain boundary) and elastic behavior for the grain boundary in the second case. The numerical calculation is carried out using the finite element method (FEM), implemented in the Zebulon calculation code. The developed approach is validated using the available experimental results reported in the literature. The numerical results showed that the estimation of TRIP given by the energetics criteria with the values of the shear deformation ( $\gamma_0 = 0.16$ ) are closer to the experiment results.

**KEYWORDS.** TRIP; Number of shear direction; Elastoplastic behavior; Martensitic transformation; Increasing load; FEM; Mono grain; Grain boundary.

OPEN ACCESS

**Citation:** M. Gaci, K. Fedaoui, L. Baroura and A. Talhi, Numerical study of TRIP transformation in 35NCD16 steel- effects of plate orientation and some criteria, *Frattura ed integrità Strutturale*, 59 (2022) 444-460.

**Received:** 01.11.2021

**Accepted:** 01.12.2021

**Published:** 01.01.2022

**Copyright:** © 2022 This is an open access article under the terms of the CC-BY 4.0, which permits unrestricted use, distribution, and reproduction in any medium, provided the original author and source are credited.

## INTRODUCTION

The deformation transformation is accompanied by an additional plastic deformation, or plasticity of transformation commonly called TRIP. This phenomenon takes place in steels solid phase change, under the application of the stress even lower than the elastic limit of austenite [1]. TRIP is observed much more in: nuclear reactor vessels, heat



treatment processes, welding, etc. [2, 4]. One of the essential characteristics to emphasize this phenomenon of plasticity transformation is its irreversible nature [5, 6 and 7].

According to Mitter [8], the phenomenon of transformation plasticity is generally explained by two mechanisms. The first presented by Greenwood-Johnson [9]; during a transformation the two phases involved (mother phase and daughter phase) do not have the same compactness (different volume). When an external stress is applied on the macroscopic scale, the plastic deformation will then be oriented. The second mechanism given by Magee [10] explains the phenomenon of TRIP in the case of martensitic transformation by the variation in volume, resulting from the formation of plates during transformation, under the effect of an external weak stress (lower than the elastic limit of austenite) [11]. Poirier [12] has defined transformational plasticity as a temporary mechanical weakening of a material, which undergoes a phase change. The following effects [13] can characterize the phenomenon; an increase in the rate of deformation, beyond the rate allowed thermally in the case of creep at constant stress and a drop in the stress, in the case of tests deformation at constant speed. Several analytical and numerical models have been proposed to satisfactorily describe the value and the kinetics of the plastic transformation flow (TRIP). These models are generally based on several micro-macro approaches, without however taking an interest in the fine evolution of the microstructure. Among the related reported work, we find Berveiller et al [14], Diani et al [15], Han et al [16], Inoue et al [17] and Ganghoffer et al [18]. In addition, these models are generally used in the case of simple types of loading and weak values of stress. Greenwood and Johnson [8], were the first to publish an interpretation relating to transformational plasticity. The Greenwood and Johnson approach was based on several hypotheses such as: The transformation is supposed to be complete, each phase is supposed to be perfectly plastic and the classical macroscopic plasticity criteria are applicable at the microscopic scale.

For the prediction of the TRIP phenomenon, Leblond [19] developed an analytical model based on the Greenwood-Johnson mechanism [8]. The model is based on a simplified micro-mechanical approach, which assumes an elastoplastic behavior of the two parent and produced phases. Other approaches were developed with the aim of a better estimation of TRIP in its two parts (kinetics and the final value) [20, 21] such as:

-A micromechanical approach [21], combining theories of limit analysis and homogenization makes possible to overcome the excessive hypotheses introduced in the Leblond model [19].

-The second approach takes into account the viscous character of the two phase's behavior (parent and produced) [23]. The purpose of this work is the analysis of the numerical simulation parameters effects on the TRIP phenomenon during martensitic transformation in 35NCD16 steel. The numerical computation is based on a micromechanical Wen model [24] using FE in two dimensions (2D) in a single grain with boundary scale. The applied mechanical loading is an increasing tensile stress in x direction with  $\sigma_{x \max} = 118$  MPa [25]. The following calculation parameters used in this study to give the order of plates formation are: the 20 shear directions of the martensitic plates (in reported works, the number of shear direction were eight [18]), the two values of the shear deformation of the martensitic plates ( $\gamma_0 = 0.16$  and  $0.19$  [26]) and the thermodynamics criteria MMDF (Max Mechanical Driving Force) [18], AMDF (Average Mechanical Driving Force) [24] and ESE (Elastic Strain Energy) [26] energetic criteria expressed in the local and global benchmarks. In the first case, elastoplastic behavior for the two domains (martensitic plate and the grain boundary) was taken into account, whereas in second case, the elastic behavior has been considered only for the grain boundary. Consequently, the influence of the numerical calculation parameters on the final value and the TRIP kinetics have been discussed and compared with the experimental results reported in the literature [25].

## THE DEFORMATION OF THE TRANSFORMATION PLASTICITY -TRIP

In the literature, the first models were not proposed until several years after the discovery of the TRIP phenomenon. The macroscopic behavior of a material can be modeled using two methods. The first is based on the thermodynamics rules for irreversible processes and the second is based on microstructural deformation mechanisms. The macroscopic behavior laws are obtained by passing from micro to macro scale [27]. For a better understanding of the TRIP phenomenon, the study of the involved physical mechanisms are necessary [28, 29]. Different authors have taken an interest in this problem by focusing on two types of tests: Cooling under stress and mechanical tests of deformation by traction, compression or torsion at constant temperature. Gautier et al. [30] observe a linear variation in the plasticity of transformation in the applied stress domain less than the elastic limit of austenite. For higher stresses, this plasticity increases rapidly. The authors find a linear variation in the plasticity of transformation in the domain of applied stress less than the elastic limit of austenite. Videau et al [31] studied the plasticity of transformation for different loading paths [6] in the case of bi-axial loadings (traction-torsion). They have shown that for the martensitic transformations, the equivalent TRIP of Von-Mises criteria is independent of the loadings type when the value of the equivalent stress was the same. The authors also conclude that the



flow direction of the transformational in plasticity is the same as the effective stress ones, which is defined as the difference between the applied external stress and internal stress of the material [31].

Greenwood and Johnson [9] have carried out several theoretical and experimental works to elucidate the phenomenon of transformation plasticity. To study the irreversible elongation during cycles with transformation, they have carried out many tests on pure iron, iron-carbon alloy, uranium, zirconium, titanium and cobalt samples. Their results show a linear relationship between the plasticity deformation of transformation and the applied stress, up to stress levels equivalent to half of the yield strength of the austenitic phase [32, 33].

The Fig. 1 shows the axial deformation measured on a tensile test piece for 16MND5 steel with and without stress dilatometer during the phase change. The application of a cooling stress during the martensitic phase change induces a residual deformation called TRIP [3]. However, in case of cooling without stress application, the TRIP phenomenon did not appear (Fig 1.b)

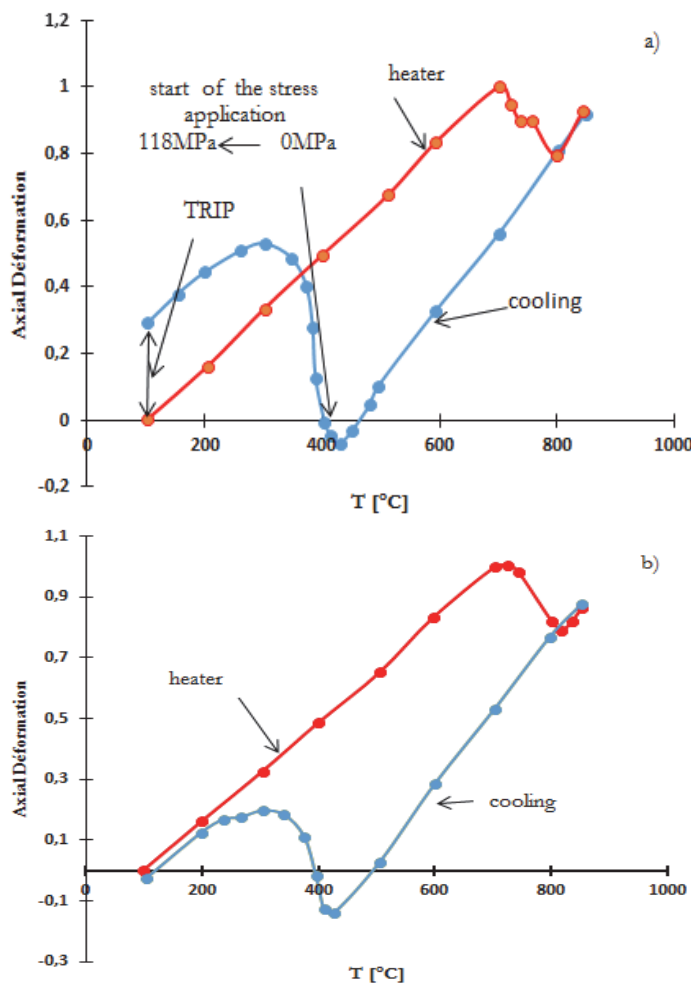


Figure 1: Axial deformation during a heating-cooling cycle (TRIP), a) under tensile stress b) stress free, [3]

## MATERIAL

In all calculations, authors consider that the martensitic phase (the daughter phase) has an elastoplastic behavior. The grain boundary follows two types of behavior, the first purely elastic and the second elastoplastic. The two phases (martensite and austenite) obey to a linear isotropic hardening model. The mechanical data used to simulate the 35NCD16 steel transformation are given in Tab. (1).

Phase's	Young's modulus (MPa)	Hardening slope (MPa)	Yield Strength (MPa)	Poisson's Ratio ( $\nu$ )
Martensite	$1.5 \times 10^5$	16500	890	0.3
Austenite	$1.8 \times 10^5$	2700	240	0.3

Table 1: Mechanical characteristics of the 35NCD16 steel [26]

To numerically simulate TRIP, Ganghoffer [18] adopts a transformation strain tensor  $\varepsilon_{(d,n)}^{tr}$  expressed by Eqn.1. The thermal deformation component tensor has two parts representing the normal dilation ( $\varepsilon_0$ ) with the plan of habitat (local reference mark d, n attached to each martensitic plate according to its orientation) and an important shearing directed along the martensitic plate ( $\gamma_0$ ), see Fig. 2. For the TRIP prediction, the tensor of thermal deformation is imposed progressively [18].

$$\varepsilon_{(d,n)}^{tr} = \begin{bmatrix} 0 & \gamma_0/2 \\ \gamma_0/2 & \varepsilon_0 \end{bmatrix} \quad (1)$$

The values of normal dilation ( $\varepsilon_0$ ) was taken equal to 0.006 and the shear deformation ( $\gamma_0$ ) measured at a temperature of 320°C was in the order of 0.16 and 0.19 [26].

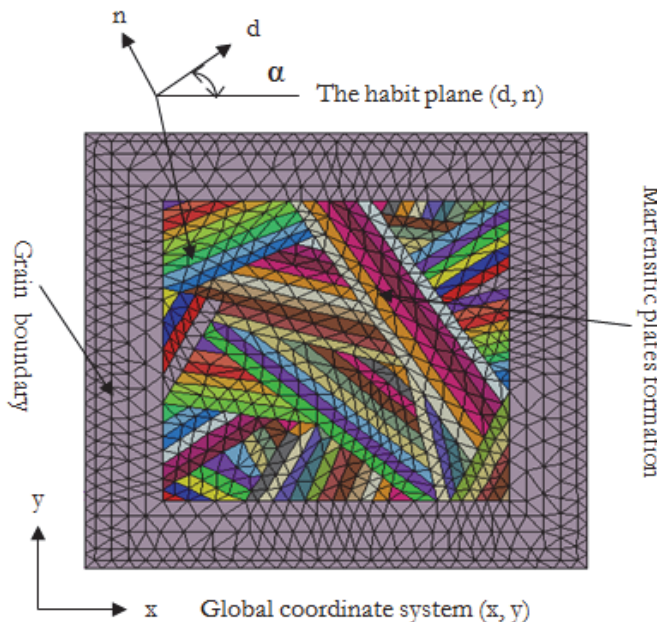


Figure 2: Mesh of the grain based on a scalene triangle

## NUMERICAL CALCULATION OF TRIP

### Geometry of the model

In this study, we used the geometry of the numerical model improved by Wen [24]. This improvement consists in creating a mesh with two areas; a contour and a central area representing respectively, the grain boundary and the formation of the martensitic plate's area. Based on the Wen's work, we have developed a mesh formed by triangular elements of scalene type (Fig. 2). Using this type of triangle in mesh construction makes possible the reach of 110 plate's in 20 possible shear directions (160°, 340°, 60°, 240°, 80°, 260°, 170°, 350°, 10°, 190°, 110°, 290°, 150°, 330°, 30°, 210°, 50°, 230°, 120° and 300°) and a contour representing the grain boundary composed of five bands. Fig. 3 shows an identification



of all the martensitic plates formed after transformation. Each plate consists of ( $N$ ) triangular element marked with a distinct color. The geometric characteristics of the plates, such as the number of elements and the shear direction ( $\alpha$ ) are given in Tab. 2.

In order to achieve a satisfactory simulation of the TRIP phenomenon, the formation domain is constituted of martensitic plates having several lengths and shear direction ( $\alpha$ ). Martensitic plates are classified into three categories according to their number of triangular elements. long plates ( $N^o$ : 41,42,43,59,60 and 64) contain between 26 and 32 triangular elements, medium plates ( $N^o$ : 44, 45, 61, 62, 63, 38, 46, 51, 16, 80, 25, 31, 37, 55, 92, 93, 94, 102, 103 and 104) composed of 12 to 24 elements and the short plates formed of less than 12 elements, see Tab. 2.

N° of plates	Number of elements	Shear direction of plates ( $\alpha$ )	N° of plates	Number of elements	Shear direction of plates ( $\alpha$ )	N° of plates	Number of elements	Shear direction of plates ( $\alpha$ )
1	2	160°	38	12	260°	75	8	30°
2	5	340°	39	7	80°	76	7	30°
3	7	160°	40	3	260°	77	7	210°
4	7	340°	41	32	340°	78	8	210°
5	6	160°	42	31	340°	79	9	210°
6	5	120°	43	27	160°	80	12	30°
7	6	150°	44	23	160°	81	4	150°
8	8	150°	45	19	340°	82	5	150°
9	3	160°	46	14	150°	83	9	330°
10	2	330°	47	10	330°	84	1	80°
11	9	50°	48	7	160°	85	2	260°
12	2	30°	49	4	340°	86	2	80°
13	8	60°	50	5	110°	87	2	260°
14	7	240°	51	12	290°	88	2	260°
15	6	50°	52	7	290°	89	2	80°
16	1	230°	53	2	80°	90	3	260°
17	5	60°	54	16	60°	91	4	80°
18	1	240°	55	12	240°	92	16	340°
19	6	60°	56	8	240°	93	14	340°
20	6	240°	57	4	60°	94	18	160°
21	5	50°	58	1	30°	95	14	340°
22	4	230°	59	33	110°	96	11	150°
23	3	60°	60	26	110°	97	9	340°
24	2	30°	61	20	290°	98	7	160°
25	14	30°	62	20	290°	99	6	340°
26	11	240°	63	24	120°	100	5	160°
27	9	60°	64	35	300°	101	2	170°
28	7	240°	65	3	10°	102	16	50°
29	5	50°	66	2	190°	103	15	50°
30	2	50°	67	3	10°	104	13	230°
31	15	170°	68	5	190°	105	11	230°
32	11	350°	69	6	10°	106	10	50°
33	8	170°	70	5	190°	107	9	50°
34	5	350°	71	5	10°	108	6	50°
35	3	150°	72	6	190°	109	3	230°
36	1	330°	73	7	10°	110	1	230°
37	16	80°	74	6	30°			

Table 2: Martensitic plates characteristic

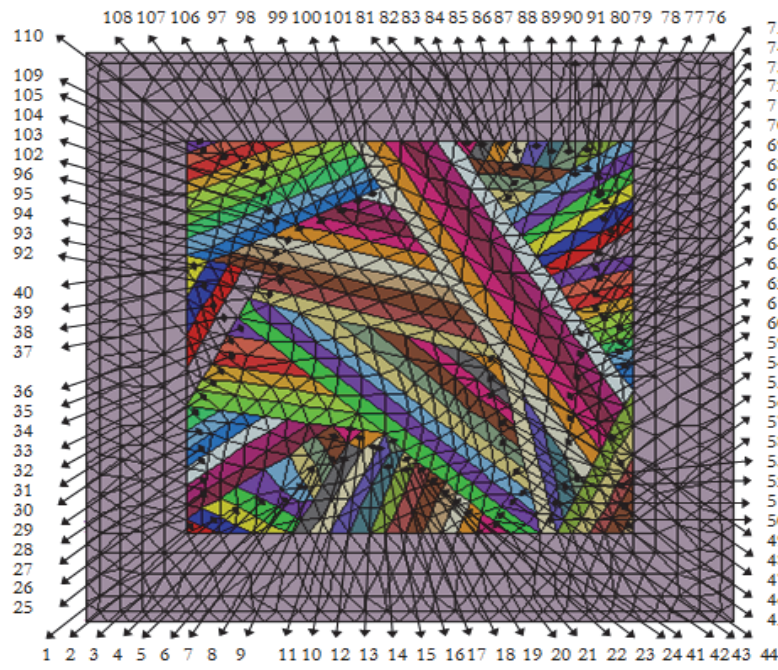


Figure 3: Identification of the martensitic plates

The calculation is carried out on the single-grain scale with boundary, under an increasing mechanical tensile stress ( $\sigma_x \text{ max} = 118 \text{ MPa}$ ), applied in the X direction, see Fig. 4 [25].

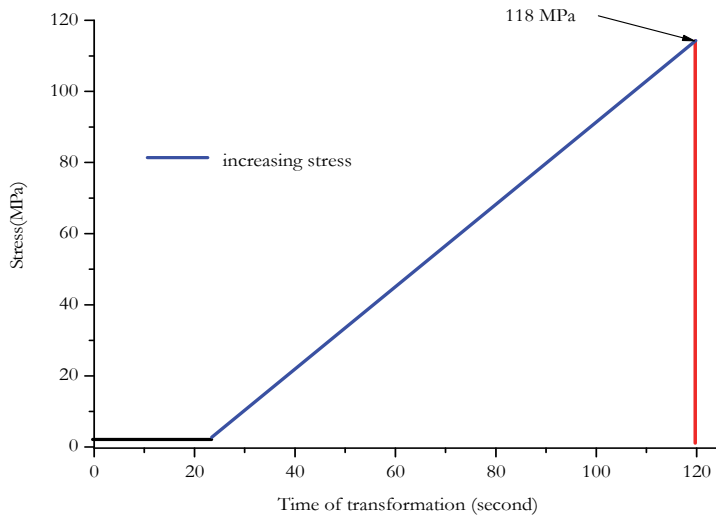


Figure 4: Presentation of the increasing tensile stress applied during the martensitic transformation [24]

#### *The advancement criteria of the martensitic transformation*

Ganghoffer [18] proposes a form of criterion based on the principles of thermodynamics, which manages the transformation of martensitic plates (Eqn. 2). This criterion is called Max Mechanical Driving Force (MMDF) [18]. The improvement of the criterion (MMDF) was carried out by Wen [23], who derived Eqn. 3, called the criterion of the Average Mechanical driving Force (AMDF).

$$\delta W_{\max} = \sigma_n \cdot \varepsilon_0 + \tau \cdot \gamma_0 \quad (2)$$



$$\delta W_{average} = \sum_{i=1}^n \delta W_i / n \quad (3)$$

where

$\delta W_{max}$  : Is the Max Mechanical Driving Force in a non-transformed mesh element (MMDF);

$\sigma_n$  : Represents the normal stress in the normal direction (n);

$\tau$  : Represents the shear stress acting in the habitat plane along the direction (d). These stresses are calculated from the state of local stress in the considered element;

$\varepsilon_0, \gamma_0$  : Represent the components of the transformation strain tensor defined in the local base (d, n), see Eqn.1 [18];

$\delta W_{average}$  : is the Average Mechanical Driving Force in the plate composed by (n) element (AMDF).

With the aim of improving qualitatively and quantitatively the results of TRIP martensitic obtained numerically, Meftah [26] used the criterion of the elastic strain energy ESE given by Eqn. 4. In addition, present numerical calculations the criterion ESE is expressed in the two local (d, n) and global (x,y) benchmarks giving LESE and GESE, respectively. Also we used the Max and Average values of this criterion to give the transformation order for each martensitic plate making up the domain.

$$\Delta E = \sum_{n=1}^{N_{el}} \left[ \sum_{i=1}^{I_{\beta}} \sigma_{ij}^t * \Delta \varepsilon_{ij}^{el(t)} \right]_{nel} \quad (4)$$

where:

$\Delta E$ : The increment of the Elastic Strain Energy (ESE) resulting from the plate transformation;

$n_{el}$ : The number of the element considered;

$N_{el}$ : The total number of elements;

$t$ : The number of the time increment considered;

$I_{\beta}$ : The number of increments necessary for the transformation of a plate;

$\Delta \varepsilon_{ij}$ : The increment of the tensor of local deformations at the moment « t »;

$\sigma_{ij}$ : The tensor of local constraint at the moment « t ».

## RESULTS AND DISCUSSION

The context of technical requirements for a better numerical prediction of TRIP under an increasing tensile stress ( $\sigma_x$  max = 118 MPa), have lead us to better consider an optimum parameters for the simulation such as: the increase of shear directions number of the martensitic plates to 20 (160 °, 340 °, 60 °, 240 °, 80 °, 260 °, 170 °, 350 °, 10 °, 190 °, 110 °, 290 °, 150 °, 330 °, 30 °, 210 °, 50 °, 230 °, 120 °, 300 °) and taking into account two shearing values  $\gamma_0 = 0.16$  and 0.19. On the other hand, two types of mechanical behavior have been used, the first considers an elastoplastic behavior for the formation of martensitic plate's area and the grain boundary, the second admits an elastic behavior for only the grain boundary (the martensitic plates behave according to the elastoplastic mode). The influence of the parameters giving the order of martensitic plate's formation in the grain (transformation advancement criteria) has been tested using the following criteria:

-MMDF (Max Mechanical Driving Force: This is the max value calculated with Eqn. 2 between all the triangular elements constituting the martensite plate in question;

-AMDF (Average Mechanical Driving Force: This is the average value calculated with Eqn. 3 between all the triangular elements constituting the martensite plate in question;

-ALESE (Average Local Elastic Strain Energy expressed in the local coordinate system (d, n): This is the average value calculated with Eqn. 4 between all the triangular elements constituting the martensite plate in question;

-MLESE (Max Local Elastic Strain Energy expressed in the local coordinate system (d, n): This is the max value calculated with Eqn. 4 between all the triangular elements constituting the martensite plate in question;

- AGESE (Average Global Elastic Strain Energy-expressed in the global coordinate system (x, y): This is the average value calculated with Eqn. 4 between all the triangular elements constituting the martensite plate in question;
- MGESE (Max Global Elastic Strain Energy-expressed in the global coordinate system (x, y): This is the max value calculated with Eqn. 4 between all the triangular elements constituting the martensite plate in question;

#### *Elastic boundary of grain and elastoplastic behavior for martensitic phase*

Figs 5 and 6 show the variation of TRIP according to the progress of the martensitic plate's formation in the grain with a purely elastic behavior of the grain boundary, while the martensitic phase obeys to an elastoplastic behavior. It can be noticed in Fig. 5.a that with the use of the two criteria AMDF ( $\gamma_0 = 0.16$ ) and MMDF ( $\gamma_0 = 0.16$ ) a completely superimposed trip kinetics has been obtained. In addition, the variation in the deformation (TRIP) was very rapid from the start to 60% of the transformation compared with the experiment results [24]. Beyond this threshold ( $Z \geq 60\%$ ) a loss of kinetics is recorded. The final values of trip obtained with the three criteria, namely AMDF ( $\gamma_0 = 0.16$ ) and MMDF ( $\gamma_0 = 0.16$ ) are almost equal and slightly lower compared to that given by the experience [25]. On the other hand, with the use of the shear deformation value  $\gamma_0 = 0.19$ , the three criteria (AMDF, MMDF) give a kinetics and the final value of trip largely estimated compared to the results of the experiment [25], see Fig 5.b.

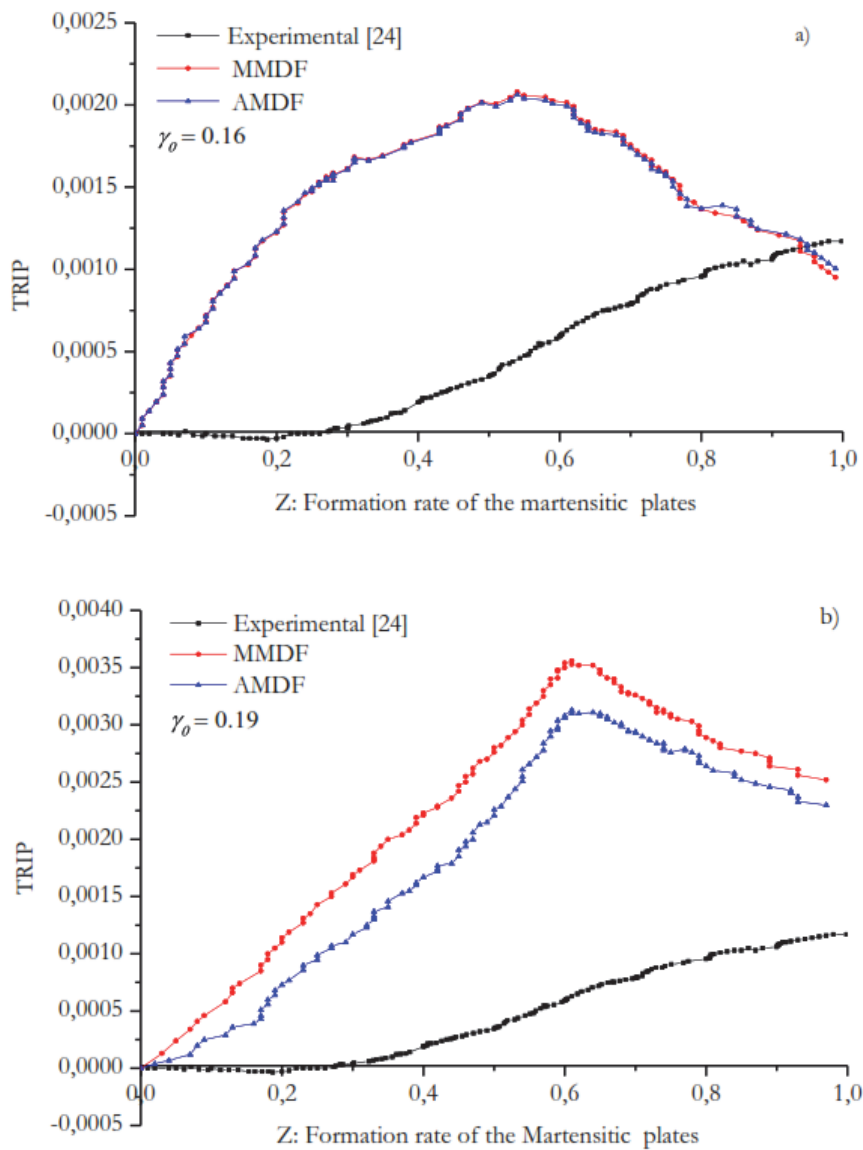


Figure 5: Evolution of TRIP under an increasing stress depending on the progress of the transformation with elastic behavior of the grain boundary and elastoplastic for martensitic phase for a)  $\gamma_0 = 0.16$ , b)  $\gamma_0 = 0.19$ .



In Fig. 6.a, we observe that the transformation kinetics obtained with the two criteria MLESE ( $\gamma_0 = 0.16$ ) and MGESE ( $\gamma_0 = 0.16$ ) were relatively better compared to the experiments [25] in the ranges of  $0\% \leq Z \leq 15\%$  and  $37\% \leq Z \leq 70\%$  for MLESE and  $37\% \leq Z \leq 60\%$  for MGESE. The average values of these two criteria ALESE ( $\gamma_0 = 0.16$ ) and AGESE ( $\gamma_0 = 0.16$ ), permit to obtain a fast TRIP kinetics from the beginning of the transformation to  $Z \leq 72\%$ . With four criteria MLESE ( $\gamma_0 = 0.16$ ), MGESE ( $\gamma_0 = 0.16$ ), ALESE ( $\gamma_0 = 0.16$ ) and AGESE ( $\gamma_0 = 0.16$ ), the final values of TRIP are significantly improved compared with those obtained with the first criteria and are almost equal to the experimental final value [24]. In the calculations where the shear deformation value  $\gamma_0$  was equal to 0.19, it can be clearly seen that the criteria MLESE ( $\gamma_0 = 0.19$ ), MGESE ( $\gamma_0 = 0.19$ ), ALESE ( $\gamma_0 = 0.19$ ) and AGESE ( $\gamma_0 = 0.19$ ) induced very fast transformation kinetics and fairly large final values of TRIP, see Fig 6.b.

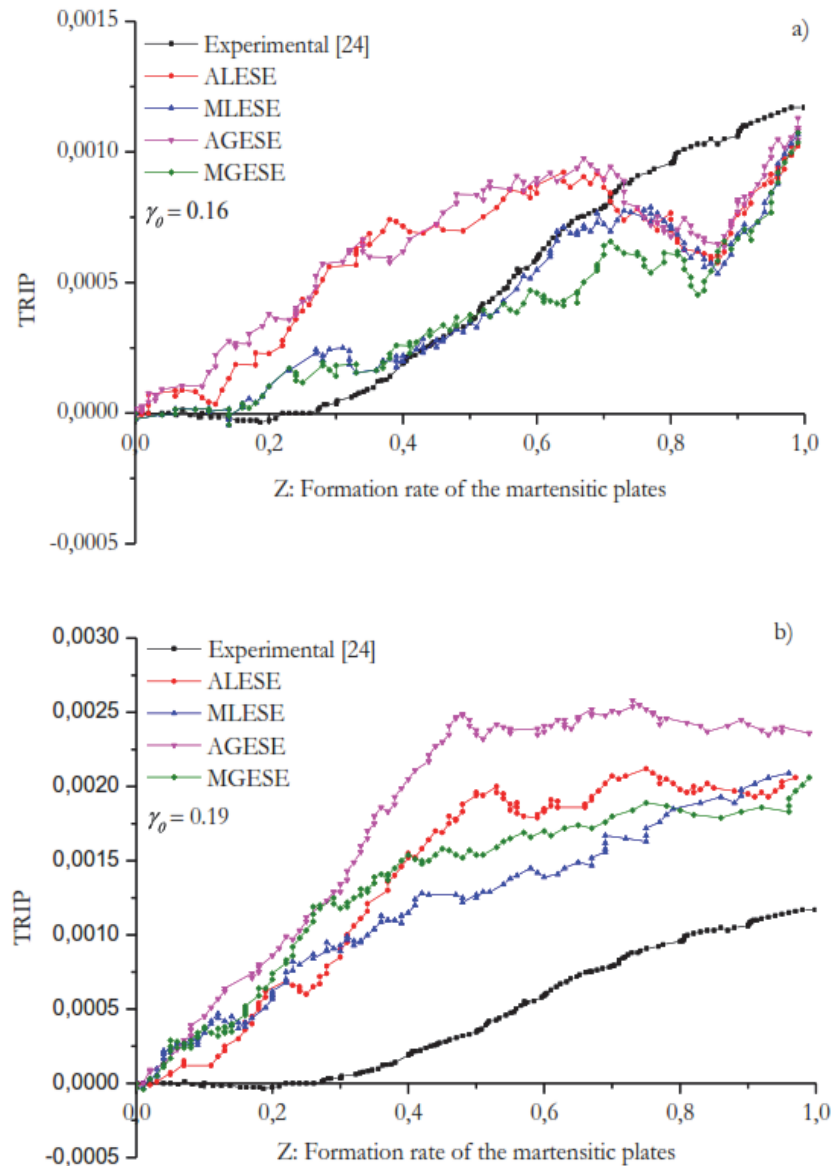


Figure 6: Evolution of TRIP under an increasing stress depending on the progress of the transformation with elastic behavior of the grain boundary and elastoplastic for martensitic phase for a)  $\gamma_0 = 0.16$ , b)  $\gamma_0 = 0.19$ .

#### Elastoplastic behavior of the grain boundary and martensitic phase

Figs. 7 present the variation of TRIP as a function of the progress of the martensitic plate's formation in the grain, with an elastoplastic behavior of the grain boundary as well as for the martensitic phase. The first remark which appears quickly is

that, the use of the shear deformation value  $\gamma_0 = 0.16$  and the criteria AMDF ( $\gamma_0 = 0.16$ ) and MMDF ( $\gamma_0 = 0.16$ ), gives the same evolution of TRIP presented in previous section, see Fig 7.a. Furthermore, it can be seen in Fig. 7.b that the curves obtained with the AMDF ( $\gamma_0 = 0.19$ ) and MMDF ( $\gamma_0 = 0.19$ ) criteria are perfectly superimposed.

Using AMDF ( $\gamma_0 = 0.19$ ) and MMDF ( $\gamma_0 = 0.19$ ) criteria, we obtain fast and linear TRIP kinetics up to  $Z = 65\%$  of martensitic plates formation. On the other hand, we find that the value of TRIP obtained at the rate of  $Z = 62\%$  was equal to 0.00355, which is much greater than obtained using the same criteria in case of the shear deformation  $\gamma_0 = 0.16$  (TRIP = 0.0022), see Fig 7. We note that the two criteria AMDF and MMDF, whether calculated with  $\gamma_0 = 0.16$  or 0.19, give a poor estimation of the TRIP, compared to the results of the experiment [25].

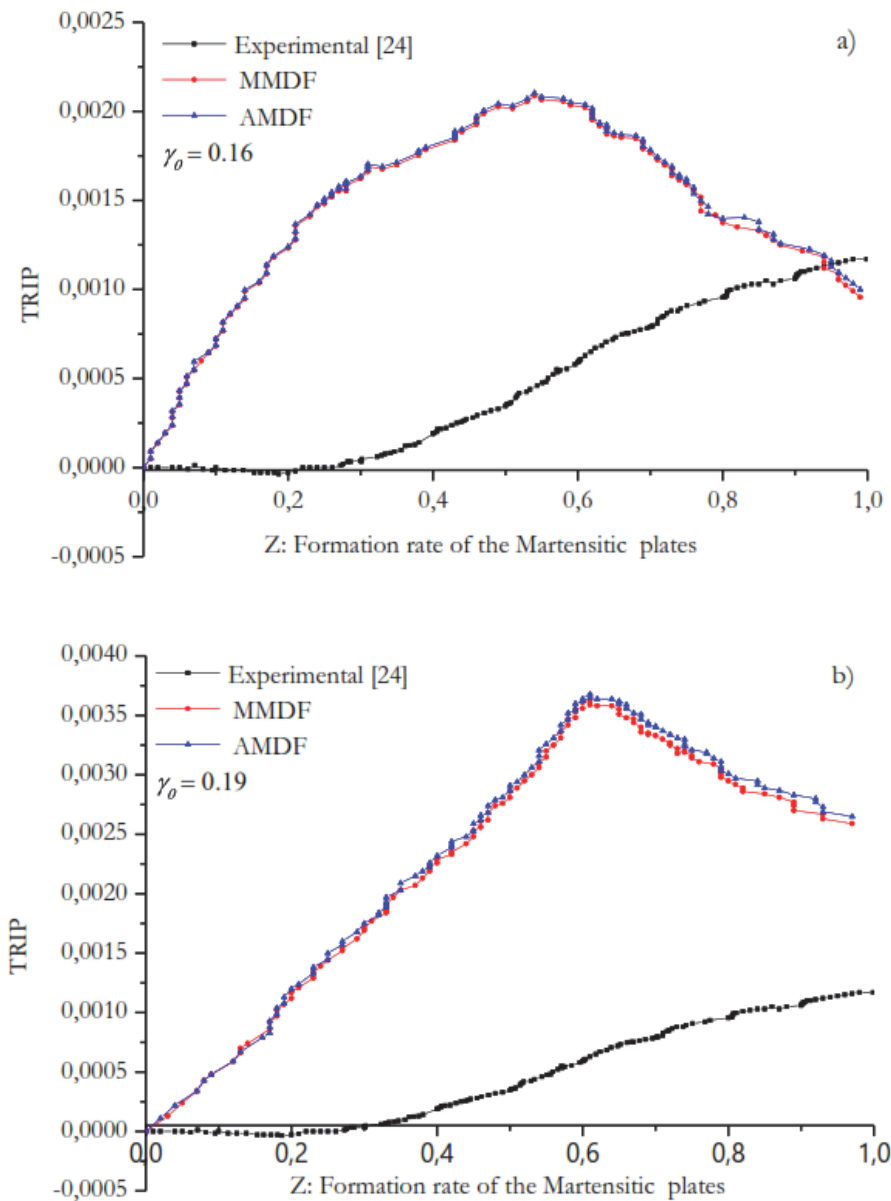


Figure 7: Evolution of TRIP under an increasing stress depending on the progress of the transformation with an elastoplastic behavior of the grain boundary and martensitic phase for a)  $\gamma_0 = 0.16$ , b)  $\gamma_0 = 0.19$ .

In Figs. 8.a we show the evolution of TRIP during martensitic transformation with the criteria for ordering the formation of platelets, such as ALESE, MLESE, AGESE and MGESE. Using the values of the shear deformation  $\gamma_0 = 0.16$ , it was found that the estimated strain is similar to that given in the fig. 6.a. In Fig. 8.b, we present the TRIP evolution obtained with the same criteria (MLESE, MGESE, AGESE and ALESE) in case of shear deformation  $\gamma_0 = 0.19$ . We notice that, the



TRIP curves obtained with the criteria ALESE and AGESE are nearly superimposed. The same behavior has been observed for two curves plotted using the criteria MLESE and MGESE. The deformation kinetics (TRIP) obtained with the criteria ALESE and AGESE was found to be faster until 50% of the rate of transformation Z where the TRIP value was about 0.0025. Beyond 50%, there is almost a stable TRIP kinetic value showing a very slight variation. The two max energy criteria MLESE and MGESE favor almost linear TRIP kinetics over the entire range of martensitic transformation ( $0\% \leq Z \leq 100\%$ ).

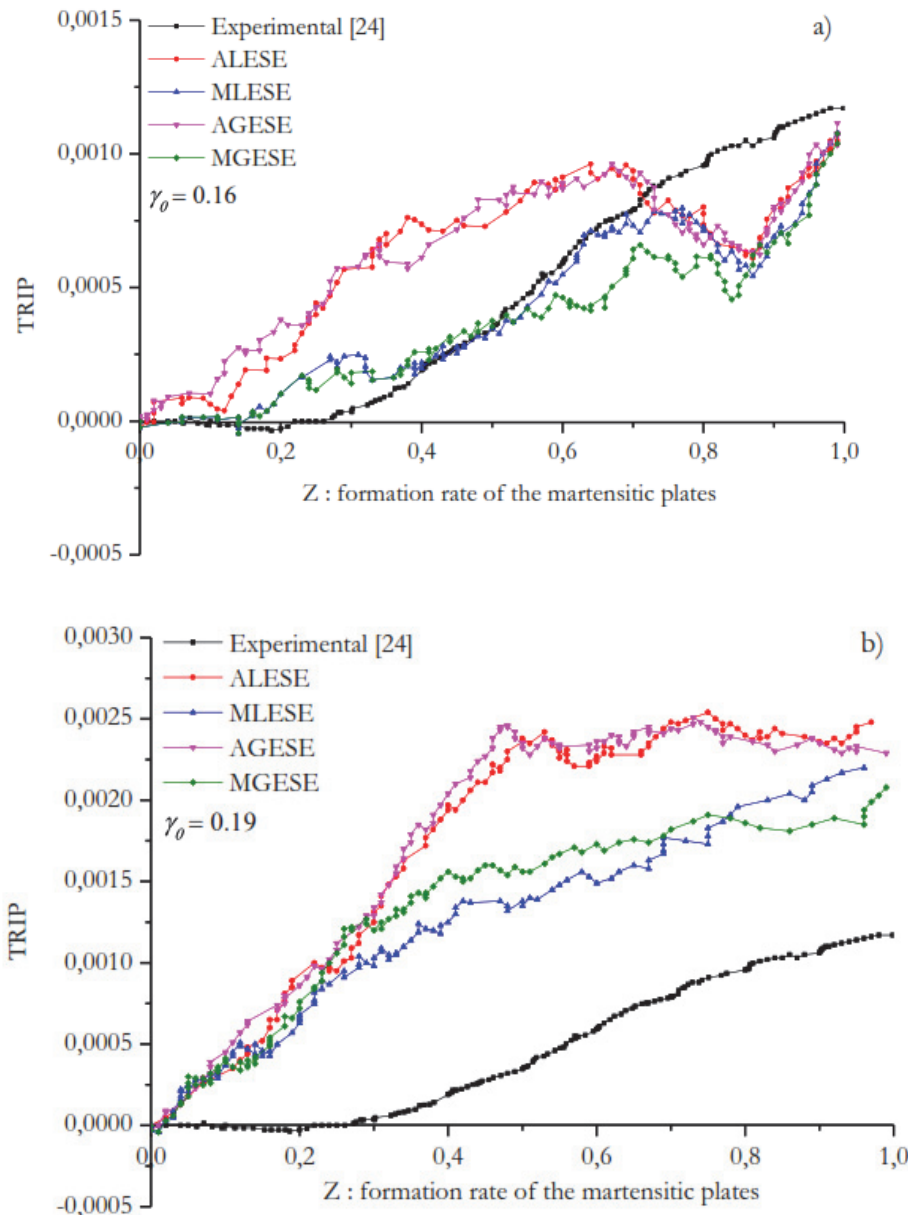


Figure 8: Evolution of TRIP under an increasing stress depending on the progress of the transformation with an elastoplastic behavior of the grain boundary and martensitic phase for a)  $\gamma_0 = 0.16$ , b)  $\gamma_0 = 0.19$ .

From the results presented in the last two sections, we observe that the two types of behavior do not give a significant difference. Whereas, the value  $\gamma_0 = 0.16$  of the shear deformation of martensitic plates favors an acceptable estimation of TRIP better than the value of  $\gamma_0 = 0.19$ . In addition, the MLESE ( $\gamma_0 = 0.16$ ) criterion presents a better estimation of the TRIP than the other criteria by referring to the experience curve [25].

transformation order for plates with criteria AMDF ( $\gamma_0 = 0.16$ )						transformation order for plates with criteria MMDF ( $\gamma_0 = 0.16$ )					
N° plates ( $\alpha$ )	Z (%)	N° plates ( $\alpha$ )	Z (%)	N° plates ( $\alpha$ )	Z (%)	N° plates ( $\alpha$ )	Z (%)	N° plates ( $\alpha$ )	Z (%)	N° plates ( $\alpha$ )	Z (%)
56 (240°)	0.00	34 (350°)		73 (10°)		56 (240°)	0.00	34 (350°)		73 (10°)	
14 (240°)		82 (150°)		67 (10°)		81 (150°)		82 (150°)		67 (10°)	
26 (240°)		1 (160°)		65 (10°)		14 (240°)		1 (160°)		65 (10°)	
28 (240°)		100 (160°)		102 (50°)		26 (240°)		100 (160°)		102 (50°)	
55 (240°)		5 (160°)		103 (50°)		28 (240°)		5 (160°)		103 (50°)	
18 (240°)		44 (160°)		109 (230°)		55 (240°)		44 (160°)		109 (230°)	
20 (240°)		3 (160°)		110 (230°)		18 (240°)		3 (160°)		110 (230°)	
63 (120°)		43 (160°)		107 (50°)		20 (240°)		43 (160°)		107 (50°)	
64 (300°)		98 (160°)		104 (230°)		63 (120°)		98 (160°)		104 (230°)	
50 (110°)		96 (150°)		106 (50°)		64 (300°)		96 (150°)		106 (50°)	
52 (290°)		94 (160°)		108 (50°)		50 (110°)		94 (160°)		108 (50°)	
51 (290°)		60 (110°)		105 (230°)		52 (290°)		60 (110°)		105 (230°)	
36 (330°)		92 (340°)		80 (30°)		51 (290°)		92 (340°)		80 (30°)	
62 (290°)		97 (340°)		78 (210°)		59 (110°)		97 (340°)		78 (210°)	
59 (110°)		99 (340°)		79 (210°)		62 (290°)		99 (340°)		79 (210°)	
61 (290°)		45 (340°)		77 (210°)		36 (330°)		45 (340°)		77 (210°)	
10 (330°)		88 (260°)		76 (30°)		61 (290°)		88 (260°)		76 (30°)	
35 (150°)		90 (260°)		74 (30°)		10 (330°)		90 (260°)		74 (30°)	
47 (330°)		87 (260°)		75 (30°)		35 (150°)		87 (260°)		75 (30°)	
81 (150°)		85 (260°)		24 (30°)		47 (330°)		85 (260°)		24 (30°)	
8 (150°)		41 (260°)		22 (230°)		8 (150°)		41 (260°)		22 (230°)	
66 (190°)		38 (260°)		54 (60°)		66 (190°)		38 (260°)		27 (60°)	
68 (190°)		40 (260°)		27 (60°)		68 (190°)		40 (260°)	0.61	54 (60°)	
70 (190°)		42 (340°)		57 (60°)		70 (190°)		42 (340°)	0.62	57 (60°)	
72 (190°)	0.62	37 (80°)		17 (60°)		72 (190°)		37 (80°)		17 (60°)	
6 (120°)		95 (340°)		19 (60°)		6 (120°)		95 (340°)		19 (60°)	
9 (160°)		53 (80°)		23 (60°)		9 (160°)		53 (80°)		23 (60°)	
46 (150°)		39 (80°)		16 (230°)		46 (150°)		39 (80°)		16 (230°)	
83 (330°)		13 (60°)		12 (30°)		83 (330°)		13 (60°)		12 (30°)	
4 (340°)		93 (340°)		58 (30°)		4 (340°)		93 (340°)		58 (30°)	
7 (150°)		49 (340°)		21 (50°)		7 (150°)		49 (340°)		21 (50°)	
2 (340°)		84 (80°)		29 (50°)		2 (340°)		84 (80°)		29 (50°)	
31 (170°)		86 (80°)		25 (30°)		31 (170°)		86 (80°)		25 (30°)	
32 (350°)		71 (30°)		15 (50°)		32 (350°)		89 (80°)		15 (50°)	
33 (170°)		89 (80°)		30 (50°)		33 (170°)		71 (30°)		30 (50°)	
48 (160°)		69 (10°)		11 (50°)		48 (160°)		91 (80°)		11 (50°)	
101(170°)		91 (80°)				101(170°)	1.00	69 (10°)			1.00

Table 3: Plates transformation order under thermodynamic criteria's AMDF ( $\gamma_0 = 0.16$ ) and MMDF ( $\gamma_0 = 0.16$ )

#### *Effects of the criteria and the martensitic plates shear angle on the TRIP estimation*

The results of the elastoplastic behavior have been considered in this section to discuss the influence of the numerical parameters (since the two modes of behavior give almost the same results). Among the studied numerical parameters, we have investigated: the influence of the shearing directions ( $\alpha$ ) of the martensitic plates as well as the criteria (AMDF, MMDF, MGSE, MLESE, AGESE and ALESE) on the estimation of the kinetics and the TRIP values in the case of the shear deformation  $\gamma_0 = 0.16$ . From Fig 7.a, we can distinguish two TRIP evolution zone. the first is located in  $0\% \leq Z \leq 61\%$  range, while the second is located in  $62\% \leq Z \leq 100\%$  range. From the beginning of the transformation ( $Z = 0\%$  to  $Z = 61\%$ ), we notice that the two thermodynamic criteria AMDF, MMDF favor the martensitic plates in their shear directions situated in the second, third and fourth quarter of the circle. ( $240^\circ, 110^\circ, 120^\circ, 290^\circ, 330^\circ, 150^\circ, 160^\circ, 170^\circ, 350^\circ, 260^\circ$ ), see Tab. 3. However, with this type of plates arrangement during transformation gives an overestimation of the kinetics and TRIP values, see Fig 7.a. In the second transformation zone ( $62\% \leq Z \leq 100\%$ ), where they appear all the directions



of the plates shear directions ( $\alpha = 10^\circ, 30^\circ, 50^\circ, 60^\circ, 80^\circ, 240^\circ, 110^\circ, 120^\circ, 290^\circ, 330^\circ, 150^\circ, 160^\circ, 170^\circ, 350^\circ, 260^\circ$ ), we notice a slight improvements, but the results remain unsatisfactory. In Fig 8.a and according to the energy criterion MLESE, we may divide the evolution of the TRIP into five zones as follows: the first ( $0\% \leq Z \leq 0.14\%$ ), the second ( $0.15\% \leq Z \leq 0.40\%$ ), the third ( $0.41\% \leq Z \leq 0.70\%$ ), the fourth ( $0.71\% \leq Z \leq 0.89\%$ ) and the fifth ( $0.9\% \leq Z \leq 100\%$ ). Tab. 4 shows that these different zones are formed with plates whose shear directions are composed of the smallest to the largest angle. Only for the last two zones, the curve of the numerical results deviates slightly from the experimental ones, which is probably due to the applied behavior mode. With the two criteria MGESE and MLESE, the same results have been almost obtain. However, with the use of MGESE, the third zone ( $0.41\% \leq Z \leq 0.52\%$ ) was shorter, see Tab. 4. From the obtained results, we may conclude that the use of the criterion (MLESE) at the local scale gives an acceptable prediction of TRIP among the other tested criteria in this study. In Tab. 5, are summarized the three TRIP evolution zones and the two energy criteria AGESE and ALESE, which have almost the same arrangement of the platelets as shown in Fig 8.a. These criteria give a non-precise TRIP estimation compared to the experimental results [25].

transformation order for plates with criteria MGESE ( $\gamma_0 = 0.16$ )						transformation order for plates with criteria MLESE ( $\gamma_0 = 0.16$ )					
N° plates ( $\alpha$ )	Z (%)	N° plates ( $\alpha$ )	Z (%)	N° plates ( $\alpha$ )	Z (%)	N° plates ( $\alpha$ )	Z (%)	N° plates ( $\alpha$ )	Z (%)	N° plates ( $\alpha$ )	Z (%)
1 (160°)	0.00	84 (80°)		32 (350°)		1 (160°)	0.00	16 (230°)	0.41	31 (170°)	
64 (300°)		29 (50°)	0.40	90 (260°)		64(300°)		18 (240°)		95 (340°)	
62 (290°)		94 (160°)	0.41	26 (240°)		62 (290°)		52 (290°)		49 (340°)	
65 (10°)		48 (160°)		9 (160°)		65 (10°)		105(230°)		90 (260°)	
63 (120°)		93 (340°)		50 (110°)		63 (120°)		28 (240°)		9 (160°)	
61 (290°)		98 (160°)		54 (60°)		61 (290°)		99 (340°)		81 (150°)	
66 (190°)		104(230°)		22 (230°)		66 (190°)		68 (190°)		19 (60°)	
60 (110°)		18 (240°)		31 (170°)		60 (110°)		94 (160°)		20 (240°)	
2 (340°)		92 (340°)		91 (80°)		36 (330°)		70 (190°)		46 (150°)	
36 (330°)		52 (290°)		7 (150°)		2 (340°)		93 (340°)		91 (80°)	
58 (30°)	0.14	45 (340°)	0.52	81 (150°)		58 (30°)	0.14	98 (160°)		7 (150°)	
37 (80°)		28 (240°)		20 (240°)		37 (80°)		104(230°)		82 (150°)	
40 (260°)	0.15	103(50°)	0.53	8 (150°)		40 (260°)	0.15	33 (170°)		48 (160°)	
3 (160°)		46 (150°)		82 (150°)		39 (80°)		69 (10°)		8 (150°)	
39 (80°)		68 (190°)		73 (210°)		3 (160°)		92 (340°)		17(60°)	
38 (260°)		97 (340°)		17 (60°)		38 (260°)		25 (30°)		47(330°)	
57 (60°)		102(50°)		74 (30°)		57 (60°)		103 (50°)		14 (240°)	
41 (340°)		70 (190°)		76 (30°)		41 (340°)		72 (190°)		73 (10°)	
4 (340°)		47 (330°)		77 (210°)		34 (350°)		97 (340°)		83 (330°)	
101(170°)		88 (260°)		11 (50°)		42 (340°)		102(50°)		74 (30°)	
5 (160°)		89 (80°)		14 (240°)		53 (80°)		85 (260°)		13 (60°)	
34 (350°)		51 (290°)		75 (30°)		56 (240°)		86 (80°)		76 (30°)	0.89
42 (340°)		72 (190°)		78 (210°)		4 (340°)		27 (60°)		77 (210°)	
53 (80°)		33 (170°)		83 (330°)		30 (50°)		23 (60°)		11 (50°)	0.90
6 (120°)		69 (10°)		13 (60°)		43 (160°)		71 (10°)		50 (110°)	
56 (240°)		96 (150°)		79 (210°)		101(170°)		55 (240°)		80 (30°)	
30 (50°)		10 (330°)		80 (30°)		35 (150°)		32 (350°)		75 (30°)	
43 (160°)		12 (30°)		110(230°)		5 (160°)		87 (260°)		78 (210°)	
35 (150°)		25 (30°)		109(230°)		6 (120°)		88 (260°)		21 (50°)	
59 (110°)		105(230°)		108 (50°)		59 (110°)		89 (80°)		79 (210°)	
49 (340°)		85 (260°)		21 (50°)		24 (30°)		51 (290°)		110(230°)	
100(160°)		86 (80°)		107 (50°)		44 (60°)		96 (240°)		109(230°)	
24 (30°)		27 (60°)		106 (50°)		67 (10°)		12 (30°)		108(50°)	
67 (10°)		23 (60°)		15 (50°)		84 (80°)		10 (330°)	0.70	107(50°)	
99 (340°)		71 (10°)		16 (230°)		29 (50°)		26 (240°)		106(50°)	
44 (60°)		55 (240°)		19 (60°)		100(160°)		54 (60°)	0.71	15 (50°)	
87 (260°)		95 (340°)				45 (340°)	0.40	22 (230°)			1.00

Table 4: Plates transformation order under energetic criteria's MGESE ( $\gamma_0 = 0.16$ ) and MLESE ( $\gamma_0 = 0.16$ )



transformation order for plates with criteria AGESE ( $\gamma_0 = 0.16$ )						transformation order for plates with criteria ALESE ( $\gamma_0 = 0.16$ )					
N° plates ( $\alpha$ )	Z (%)	N° plates ( $\alpha$ )	Z (%)	N° plates ( $\alpha$ )	Z (%)	N° plates ( $\alpha$ )	Z (%)	N° plates ( $\alpha$ )	Z (%)	N° plates ( $\alpha$ )	Z (%)
65 (10°)	0.00	2 (340°)		35 (150°)		1 (160°)	0.00	40 (260°)		49 (340°)	
66 (190°)		60 (110°)		73 (10°)		65 (10°)		38 (260°)		93 (340°)	
67 (10°)		3 (160°)		47 (330°)		67 (10°)		36 (330°)		9 (160°)	
68 (190°)		92 (340°)		49 (340°)		68 (190°)		104(230°)		10 (330°)	
69 (10°)		105 (230°)		75 (30°)		66 (190°)		103(50°)		35 (150°)	
58 (30°)		41 (340°)		55 (240°)		58 (30°)		72 (190°)		34 (330°)	
70 (190°)		94 (160°)		50 (110°)		30 (50°)		51 (290°)		55 (240°)	
56 (240°)		96 (150°)		34 (330°)		64 (300°)		2 (340°)		31 (170°)	
30 (50°)		97 (340°)		33 (170°)		56 (240°)		60 (110°)		32 (350°)	
64 (300°)		43 (160°)		101(170°)		69 (10°)		92 (340°)		33 (170°)	
63 (120°)		98 (160°)		31 (170°)		63 (120°)		3 (160°)		101(170°)	
54 (60°)		110(230°)		32 (350°)		28 (240°)		43 (160°)		73 (10°)	
71 (10°)		99 (340°)		76 (30°)		26 (240°)		41 (340°)		50 (110°)	
29 (50°)		5 (160°)		24 (30°)		70 (190°)		94 (160°)		75 (30°)	0.88
25 (30°)		44 (160°)		85 (260°)	0.89	25 (30°)		96 (150°)		24 (30°)	
28 (240°)		103 (50°)		88 (260°)		29 (50°)		97 (340°)		77 (210°)	
89 (80°)		100(160°)		77 (210°)		54 (60°)		44 (160°)		23 (60°)	0.89
62 (290°)		81 (150°)		22 (230°)		62 (290°)		98 (160°)		76 (30°)	
57 (60°)		104(230°)		87 (260°)		74 (30°)		110(230°)		19 (60°)	
37 (80°)		4 (340°)		91 (80°)		61 (290°)		5 (160°)		20 (240°)	
74 (30°)		45 (340°)		20 (240°)		37 (80°)		99 (340°)		15 (50°)	
26 (240°)		7 (150°)		11 (50°)		71 (10°)		42 (340°)		22 (230°)	
61 (290°)		42 (340°)	0.68	21 (240°)		27 (60°)		81 (150°)	0.68	80 (30°)	
39 (80°)		13 (60°)		19 (60°)		57 (60°)		100(160°)		11 (50°)	
90 (260°)		46 (150°)		23 (60°)		39 (80°)		45 (340°)		14 (240°)	
53 (80°)		48 (160°)		78 (210°)		53 (80°)		46 (150°)		17 (60°)	
38 (260°)		6 (120°)		17 (60°)		108(50°)		13 (60°)		86 (80°)	
40 (260°)		102(50°)	0.69	80 (30°)		52 (290°)		4 (340°)	0.69	89 (80°)	
27 (60°)		82 (150°)		14 (240°)		107(50°)		7 (150°)		84 (80°)	
109(230°)		51 (290°)		15 (50°)		106(50°)		48 (160°)		78 (210°)	
107(50°)		10 (330°)		79 (210°)		105(230°)		82 (150°)		16 (230°)	
59 (110°)		36 (330°)		84 (80°)		59 (110°)		6 (120°)		91 (80°)	
108(50°)		95 (340°)		12 (30°)		109(230°)		83 (330°)		12 (30°)	
72 (190°)		83 (330°)		86 (80°)		87 (260°)		102(50°)		18 (240°)	
106(50°)		8 (150°)		16 (230°)		90 (260°)		47 (330°)		79 (210°)	
1 (160°)		93 (340°)		18 (240°)		85 (260°)		95 (340°)		21 (240°)	
52 (290°)		9 (160°)				88 (260°)		8 (150°)			

Table 5: Plates transformation order under energetic criteria's AGESE ( $\gamma_0 = 0.16$ ) and ALESE ( $\gamma_0 = 0.16$ )

The distribution of the shear stress  $\text{sig12}$  over all the studied grain mesh (made of the formation domain of the martensitic plates and the grain boundary) is shown in Fig. 9. However, in case of an elastoplastic behavior and with the value of  $\gamma_0 = 0.16$  in AMDF criterion, The first transformed platelets have been observed at the early stage of the transformation (time = 11.5), see Tab.3 (N°: 56,14,26,28,55,18,20,63,64,50,52,51), which generate the greatest shear stress in the area of martensitic plates formation. This observation is confirmed by the reported Magee [10] studies, which show that the martensitic transformation is favored by the shearing phenomenon.

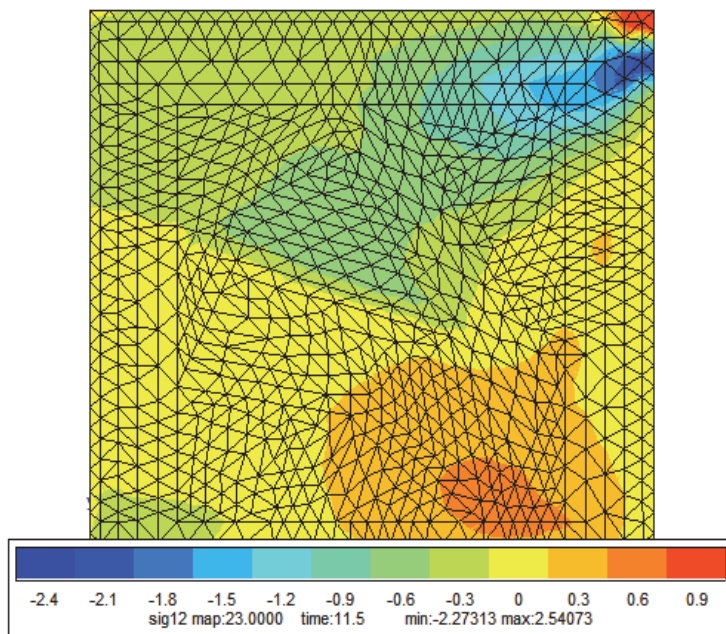


Figure 9: shear stress distribution ( $\sigma_{12}$ ) during the martensitic plate's formation with AMDF ( $\gamma_0 = 0.16$ ) criteria

## CONCLUSION

The aim of this reported work is to obtain a more rigorous and reliable numerical TRIP simulation of a martensitic transformation in 35NCD16 steel under increasing tensile stress ( $\sigma_x$  max = 118 MPa). This have been achieved by the adaptation of the parameters introduced in the numerical calculation such as: the increase in the number of shear directions (twenty directions), the use of seven criteria to give the order of plate transformation, the mono grain model with regular grain boundary and an elastic and elstoplastic behavior of the austenitic and martensitic phases. The TRIP numerical results have been compared with those reported in the literature [24]. From the obtained results, we may conclude that with the use of shear deformation  $\gamma_0 = 0.16$ , the numerical results were better than those evaluated with  $\gamma_0 = 0.19$ . The estimation values of TRIP (in its final values and kinetics) given by the MLESE ( $\gamma_0 = 0.16$ ) and MGESE ( $\gamma_0 = 0.16$ ) criteria are closer to the experiment results [25]. According to the numerical results and for a better prediction of the TRIP, it is necessary to consider a mixed behavior of mode (elastoplastic and a viscous), which may be applied in certain part of the transformation. Using the investigated numerical parameters in this study, the two types of behavior have shown almost no difference.

## REFERENCES

- [1] Fischer, F. D., Reisner, G. (1998). A criterion for the martensitic transformation of a micro region in an elastic-plastic material, *Acta Materialia*, 46(6), pp. 2095-2102.
- [2] Iesman, A.V., Levitas, V.I., Preston, D.L., Cho, J.Y. (2005). Finite element simulations of martensitic phase transitions and microstructures based on a strain softening model, *Journal of the Mechanics and Physics of Solids*, 53, pp.495-523. DOI: 10.1016/j.jmps.2004.10.001.
- [3] Valance, S., Coret, M., Combescure, A. (2007). Strain simulation of steel during a heating-cooling cycle including solid-solid phase change, *European Journal of Mechanics-A/Solids*, 26(3), pp.460-473, DOI: 10.1016/j.euromechsol.2006.11.001.
- [4] Ferro, P., Bonollo, F., Berto, F., Montanari, A. (2019). Numerical modelling of residual stress redistribution induced by TIG-dressing. *Frattura ed Integrità Strutturale*, 47, pp. 221-230.
- [5] Zhong, H., Wang, Z., Gan, J., Wang, X., Yang, Y., He, J., Wei, T.T., Qin, X. (2020). Numerical simulation of martensitic transformation plasticity of 42CrMo steel based on spot continual induction hardening model, *Surface and Coatings Technology*, 385, DOI: 10.1016/j.surfcoat.2020.125428.



- [6] Leblond, J.B., Devaux, J.C. (1989). Mathematical modeling of transformation plasticity in steels I: case of ideal-plastic phases, *Int. J. Plast.*, 5, pp. 551-572, DOI: 10.1016/0749-6419(89)9001-6.
- [7] Hazar, S., Alfredsson, B., Lai, J. (2018). Mechanical modeling of coupled plasticity and phase transformation effects in a martensitic high strength bearing steel, *Mechanics of Materials*, 117, pp. 41-57, DOI: 10.1016/j.mechmat.2017.10.001.
- [8] Mitter, W. (1987). Umwandlungsplastizität und ihre Berücksichtigung bei der Berechnung von Eigenspannungen, Berlin, Materialkundlich-Technische Reihe 7, ISBN3443230083, 276p.
- [9] Greenwood, G.W., Johnson, R. H. (1965). The deformation of metals under small stresses during phase transformation, *Proc Roy Soc*, 283, pp.403-422. DOI:10.1098/rspa.1965.0029.
- [10] Magee, C. L. (1970). Nucleation of martensite, phases transformations. ASM, Metals Park.
- [11] El Majaty, Y., Leblond, J.B., Brenner, R. (2018). Une approche micromécanique renouvelée du mécanisme de greenwood-johnson de la plasticité de transformation des métaux et alliages, Colloque national MECAMAT Aussois (Matériaux Numériques), Aussois, France.
- [12] Poirier, J.P. (1982). On transformation plasticity, *J. Geophy. Res.*, 87, pp. 6791-6797, DOI: 10.1029/jb087ib08p06791.
- [13] Behrens, B.A., Bouguecha, A., Bonk, C., Chugreev, A. (2017). Experimental investigations on the transformation-induced plasticity in a high tensile steel under varying thermo-mechanical loading, *CMMS*, 17(1), pp. 36 -43.
- [14] Berveiller, M., Zaoui, A. (1983). Modelling of the plasticity and the texture development of two-phase metals, *Proceeding of the 4th Riso Int. Symp. On Metallurgy and Materials Science*, Roskilde, Danemark, pp. 153-160.
- [15] Diani, J.M., Sabar, H., Berveiller, M. (1995). Micromechanical modelling of the transformation induced plasticity (TRIP) phenomenon in steels, *Int. J. Eng. Sci.*, 33(13), pp. 1921- 1934, DOI: 10.1016/0020-7225(95)00045-Y.
- [16] Han, H.N., Lee, C.G., Oh, C.S., Lee, T.H., Kim, S.J. (2004). A model for deformation behavior and mechanically induced martensitic transformation of metastable austenitic steel, *Acta Materialia*, 52(17)4, pp. 5203-5214, DOI: 10.1016/j.actamat.2004.07.031.
- [17] Inoue, T., Wang, Z. (1985). Coupling between stress, temperature, and metallic structures during processes involving phase transformations. *Mater. Sci. Technol.* 1, pp. 845-849, DOI: 10.1179/mst.1985.1.10.845.
- [18] Ganghoffer, J.F., Simonsson, K. (1998). A micromechanical model of the martensitic transformation, *Mechanics Materials*, 27, pp. 125-144, DOI: 10.1016/S0167-6636(97)00044-6.
- [19] Leblond, J.C., Mottet, G.J., Devaux, C. (1986). A theoretical and numerical approach to the plastic behavior of steels during phase transformations - II. Study of classical plasticity for ideal-plastic phases, *Journal Mechanical Physics Solids*, 34(4), pp. 411-432, DOI: 10.1016/0022-5096(86)90010-4.
- [20] Ahluwalia, R., Mikula, J., Laskowski, R., Quek, S. S. (2020). Phase field simulation of martensitic-transformation-induced plasticity in steel, *Phys. Rev. Materials*, 4, 103607, DOI: 10.1103/PhysRevMaterials.4.103607.
- [21] Hossain, M.A., Baxevanis, Th. (2021). A Finite Strain Thermomechanically-Coupled Constitutive Model for Phase Transformation and (Transformation-Induced) Plastic Deformation in NiTi Single Crystals; *International Journal of Plasticity*, DOI:10.1016/j.ijplas.2021.102957.
- [22] Fischer, F.D., Reisnerb, G., Wernerb, E., Tanakac, K., Cailletaudd, G., Antretterea, T. (2000). A new view on transformation induced plasticity (TRIP), *International Journal of Plasticity*, 16(7-8), pp. 723-748, DOI: 10.1016/S0749-6419(99)00078-9.
- [23] Gaubert, A., Lebouar, Y., Finel, A. (2010) Coupling phase field and visco-plasticity to study rafting in Ni-base superalloys, *Phil. Mag.*, 90 (1), pp. 375-404, DOI: 10.1080/14786430902877802.
- [24] Wen, Y.H., Denis, S., Gautier, E. (1996). Criterion for the progress of martensitic transformation in a finite element simulation, *Journal de physique*, IV (J. phys., IV), *Colloque C2*, 5, 531.pp. 146, DOI: 10.1051/jp4.
- [25] Tahimi, A., Taleb, L., Barbe, F. (2009). Plasticité induite par transformation de phase martensitique dans l'acier 35NCD16, 19ème Congrès Français de Mécanique, Marseille, France.
- [26] Meftah, S., Barbe, F., Taleb L., Sidoroff, F.(2007). Parametric numerical simulations of TRIP and its interaction with classical plasticity in martensitic transformation, *European Journal of Mechanics - A/Solids*, 26(4), pp.688-700.
- [27] Polatidis, E.G., Haidemenopoulosb, N., Krizanc, D., Aravasbd, N., Panznerae, T., Šmídf, M., Papadiotib, I., Casatif, N., Petegemf, V., VanSwygenhovenfg, H. (2021). The effect of stress triaxiality on the phase transformation in transformation induced plasticity steels: Experimental investigation and modelling the transformation kinetics, *Materials Science and Engineering*, 800, 40321, DOI: 10.1016/j.msea.2020.140321.
- [28] Hazara, S., Alfredsson, Bo., Laib, J. (2018). Mechanical modeling of coupled plasticity and phase transformation effects in a martensitic high strength bearing steel, *Mechanics of Materials*, 117, pp. 41-57, DOI: 10.1016/j.mechmat.2017.10.001.



- [29] Barbe, F., Quey, R., Taleb, L., Souza, D.C. (2008). Numerical modelling of the plasticity induced during diffusive transformation. An ensemble averaging approach for the case of random arrays of nuclear, European Journal of Mechanics A/Solids, 27, DOI: 10.1016/j.euromechsol.2008.01.005.
- [30] Gautier, E., Zhang, J. S., Zhang, X. M. (1995). Martensitic transformation under stress in ferrous alloys. Mechanical behaviour and resulting morphologies, J. Phys. IV, 5(8), pp. 8-41, DOI: 10.1051/ip4:1995805.
- [31] Videau, J.C., Cailletaud, G., Pineau, A. (1996). Experimental study of the transformation-induced plasticity in a Cr-Ni-Mo-Al-Ti steel, J. Phys. IV, 6(C1), pp. 1-465.
- [32] Taleb, L., Sidoroff, F. (2003). A micromechanical modeling of Greenwood-Johnson mechanism in transformation induced plasticity, Int. J. Plasticity, 19 (10), pp. 1821- 1842, DOI: 10.1016/S0749-6419(03)00020-2.
- [33] Soleimani, M., Rezakalhor, A., Mirzadeh, H. (2020). Transformation-induced plasticity (TRIP) in advanced steels, Materials Science and Engineering: A, 795, 140023, DOI: 10.1016/j.msea.2020.140023.